Six coordinate dinuclear lanthanide(III) amide complexes: Investigation of magnetization Relaxation dynamics and their electronic structures

Amaleswari Rasamsetty,[a] Sakshi Mehta,[b] Kamal Uddin Ansari,[a] Pradeep Kumar,[a] Abhishake Mondal*[b] and Maheswaran Shanmugam*[a]

[a]*Department of Chemistry, Indian Institute of Technology Bombay, Powai, Mumbai-400076, Maharashtra, India. Email: eswar@chem.iitb.ac.in*

[b] *Solid State and Structural Chemistry Unit, Indian Institute of Science, Sir C V Raman Road, Bangalore 560012, India. E-mail: mondal@iisc.ac.in*

EXPERIMENTAL SECTION

Materials and General Methods.

Unless otherwise stated, all reactions were carried out under an inert (Argon) atmosphere. The ***Lithium 2,6-Diisopropyl-N-(trimethylsilyl)anilide*** (L) ligand was prepared using the literature method.[1] THF and hexane solvents were dried with sodium and benzophenone and distilled prior to use.[2] All other chemicals were purchased from commercially available sources (Alfa Aesar and Sigma-Aldrich). ^{1}H NMR and ^{29}Si spectra were recorded on a Bruker Avance III 500. Single-crystal data were collected on a Rigaku Saturn CCD diffractometer using a graphite monochromator (Mo Kα, $\lambda = 0.71073$ Å). The selected crystals were mounted on the tip of a glass pin using mineral oil and placed in the cold flow produced with an Oxford Cryo-cooling device. Complete hemispheres of data were collected using ω and φ scans (0.3°, 16 s per frame). Integrated intensities were obtained with Rigaku Crystal Clear-SM Expert 2.1 software, and they were corrected for absorption correction. Structure solution and refinement were performed with the SHELX package.[3] The structures were solved by direct methods and completed by iterative cycles of ΔF syntheses and full-matrix least-squares refinement against F^2. Elemental analysis (C, H, and N) were carried out using a Thermo-quest micro-analyzer spectrometer. The magnetic susceptibility measurements were performed with Quantum Design MPMS-XL EverCool SQUID magnetometer, between 1.9 K and 280 K for dc applied fields ranging from -5 to 5 T. Polycrystalline sample of **1** (18.6 mg) and **2** (10.8 mg) were introduced in a polyethylene bag ($2.8 \times 0.65 \times 0.025$ cm) were subjected to measurements. The temperature-dependent data were measured using 1000 Oe and 10000 Oe. The isothermal magnetization data were acquired between 1.9 and 32 K for **1** and 1.9 and 8 K for **2**. *M vs H* measurements was performed at 100 K to check for the presence of ferromagnetic impurities which were found to be absent. The magnetic data were corrected for the sample holder and the diamagnetic contribution. The *ac* susceptibility measurements were measured with an oscillating *ac* field of 3.5 Oe with frequency between 1 to 1500 Hz using MPMS-XL EverCool SQUID magnetometer. Both complexes **1** and **2** are air and moisture sensitive, so the sample was prepared using a sealed bag inside the glove box under an argon atmosphere. Systematic analysis of the coordination geometries around the metal atoms were identified using SHAPE 2.1 software.[4]

General Synthetic Procedure for complexes 1 - 3 $[\mathrm{Ln_2}(\mu\text{-Cl})_2\mathrm{Cl_4Li_2(L)_2(THF)_6}]$:

Ligand (L) (1.5 eq.) was dissolved into 10 ml of dry THF in a Schlenk tube. Anhydrous $LnCl_3$ (1 eq.) was added into the reaction mixture and it was stirred at room temperature for 12 hours. After stirring it for 12 hours THF was evaporated under vacuum and the target compound was extracted with dry hexane (5 mL) and it was filtered and left for the crystallization at -25 °C. Colourless crystals were formed within 3 days which are suitable for single crystal X-ray diffraction.

Complex **1**. L (0.15 g, 0.566 mmol), was dissolved into 10 ml of dry THF, anhyd. $GdCl_3$ (0.10 g. 0.377 mmol) was added left it for stirring 12 hrs. After extraction in to hexane colourless crystals were formed within 3 days at -25 °C. Yield: 0.10 g (based on Gd 26.33%). Elemental analysis Calculated (%): C, 44.10; H, 6.85; N, 1.90. Observed (%) C, 44.07; H, 6.69; N, 2.35. IR (cm^{-1}): 3089w, 3024w, 2787w, 2738w, 1606m, 1504w, 1402m, 1375m, 1208s, 1070s, 990w, 831w, 796s, 758s, 668m.

Complex **2**. L (0.15 g, 0.566 mmol), was dissolved into 10 ml of dry THF, anhyd. $DyCl_3$ (0.101 g. 0.377 mmol) was added left it for stirring 12 hrs. After extraction into hexane colourless crystals were formed within 3 days at -25 °C. Yield: 0.080 g (based on Dy 26.33%). Elemental analysis Calculated (%): C, 43.79; H, 6.80; N, 1.89. Observed (%) C, 43.49; H, 6.63; N, 2.10. IR (cm^{-1}): 3069w, 3015w, 2793w, 2715w, 1597m, 1496w, 1378m, 1207s, 1069s, 970w, 815w, 776s, 718s, 644m.

Complex **3**. L (0.15 g, 0.566 mmol), was dissolved into 10 ml of dry THF, anhyd. YCl_3 (0.073 g. 0.377 mmol) was added left it for stirring 12 hrs. After extraction in to hexane colourless crystals were formed within 3 days at -25 °C. Yield: 0.09 g (based on Y 36.14%). Elemental analysis Calculated (%): C, 48.68; H, 7.56; N, 2.10. Observed (%) C, 49.40; H, 7.60; N, 2.49. IR (cm^{-1}): 3080w, 3031w, 2811w, 2730w, 1594m, 1492w, 1399m, 1210s, 1084s, 995w, 873w, 795s, 750s, 694m.

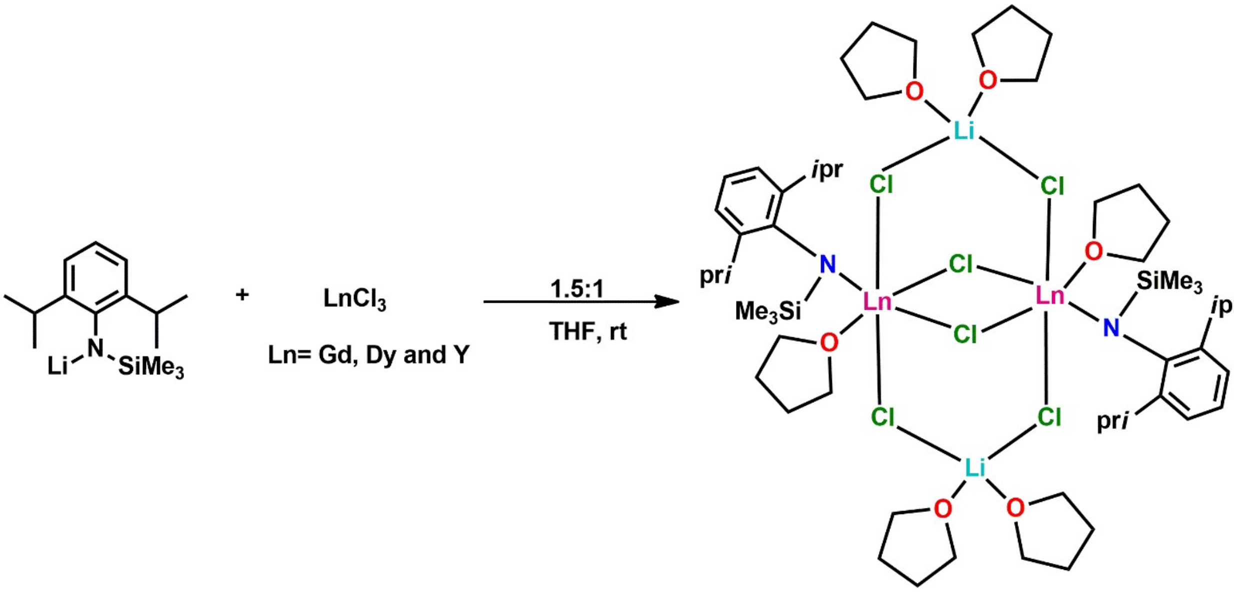

Scheme-S1: The general synthetic procedure followed to isolate complexes **1 - 3**.

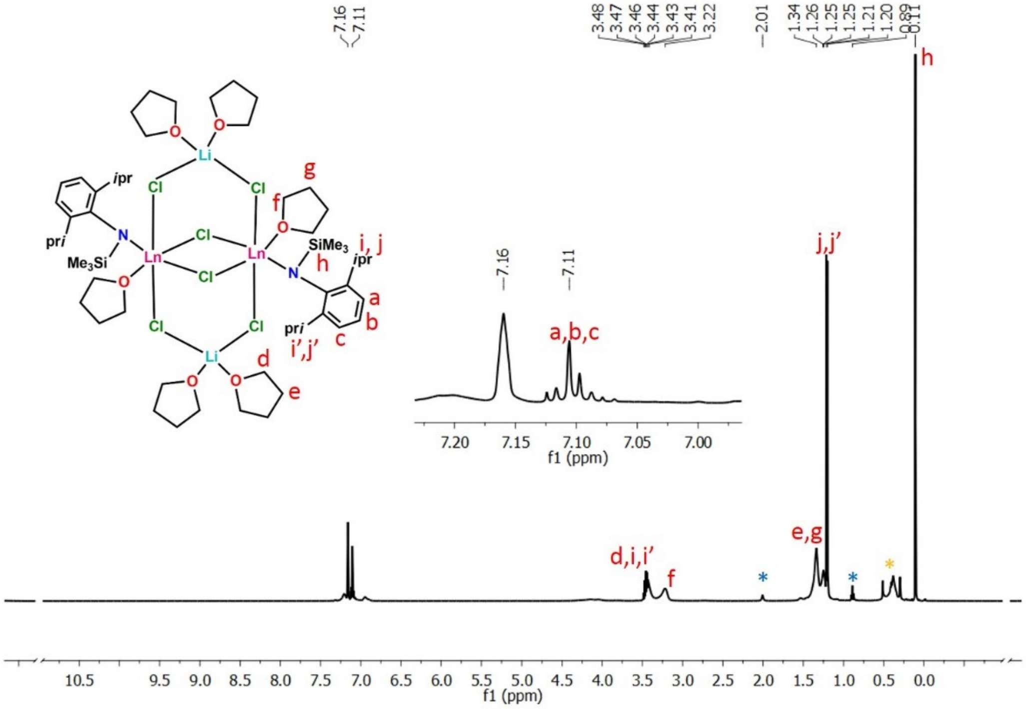

Figure S1: ^{1}H-NMR spectrum of complex **3** recorded at room temperature in C_6D_6. (*-hexane and *grease)

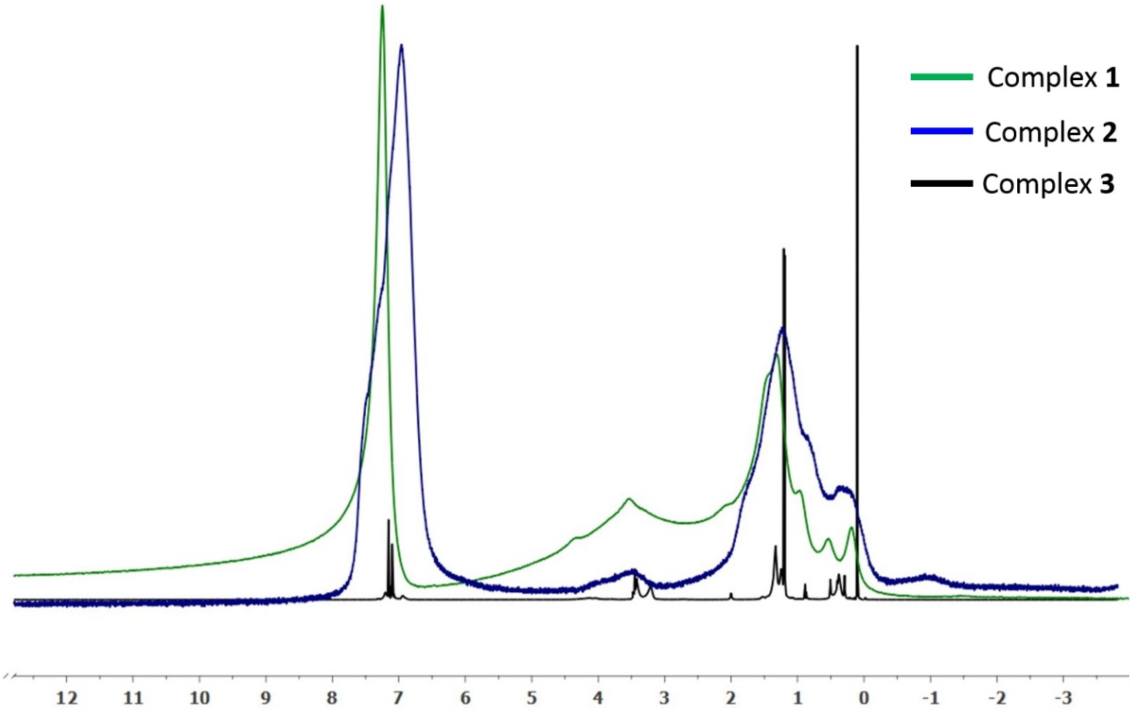

Figure S2: Overlay of ^{1}H-NMR spectra of complexes **1-3** recorded at room temperature in C_6D_6 shown above to confirm the purity of the complexes.

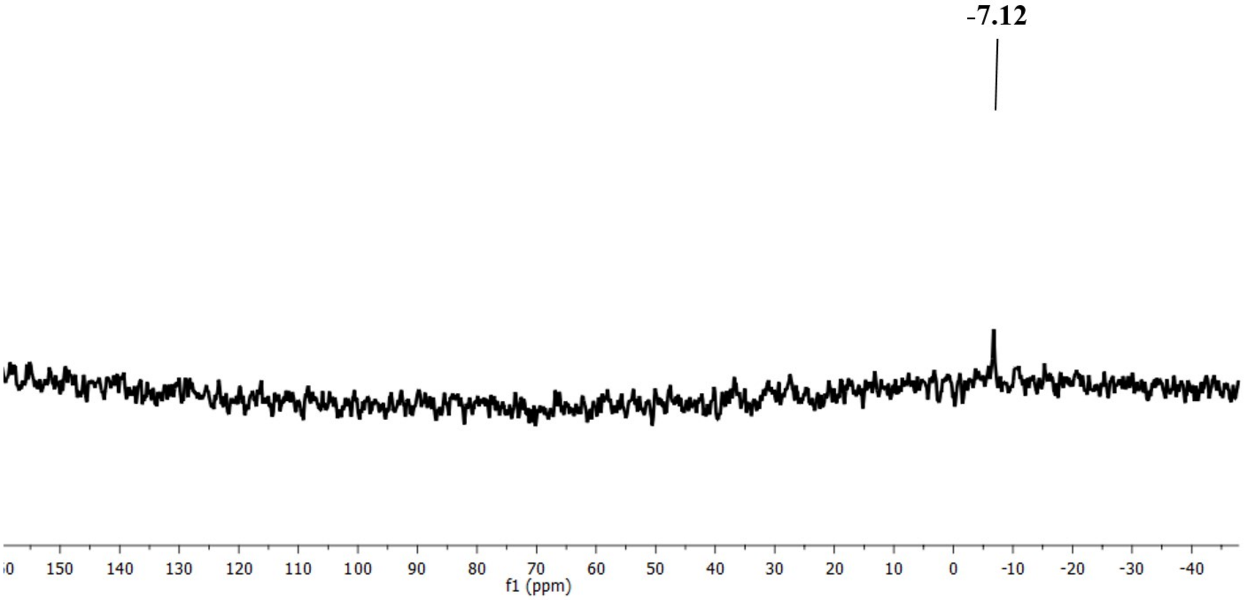

Figure S3: ^{29}Si-NMR spectrum of complex **3** recorded at room temperature in C_6D_6**.**

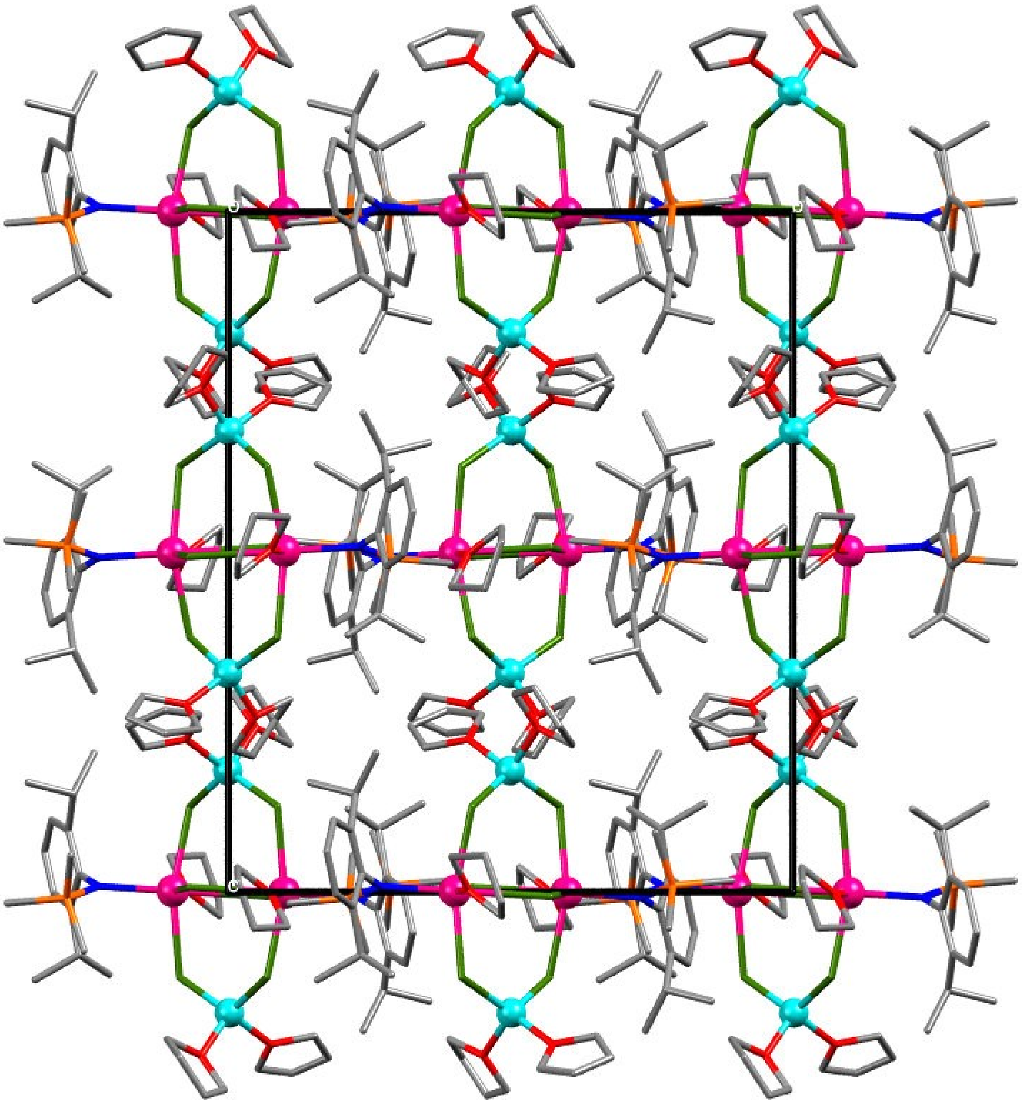

Figure S4: Packing diagram of complex **1** (view along b-axis). Colour code: Pink = Gd(III), blue = N, grey = C, Cyan= Li, Green = Cl, Orange = Silicon and Red = O.

Table S1: Crystallographic parameters for the complexes **1-3.**

	1	**2**	**3**
Empirical formula	$C_{54}H_{100}Cl_6Gd_2Li_2N_2O_6Si_2$	$C_{54}H_{100}Cl_6Dy_2Li_2N_2O_6Si_2$	$C_{54}H_{100}Cl_6Y_2Li_2N_2O_6Si_2$
Fw.g mol^{-1}	1470.61	1481.11	1333.93
Crystal system	orthorhombic	orthorhombic	orthorhombic
Space group	Pbca	Pbca	Pbca
a/Å	18.9685(3)	18.8807(2)	18.8863(14)
b/Å	17.2945(3)	17.2088(2)	17.2224(17)
c/Å	20.8481(5)	20.8678(3)	20.8711(19)
α (°)	90	90	90
β (°)	90	90	90
γ(°)	90	90	90
v/Å	6839.2(2)	6780.25(15)	6788.7(11)
Z	4	4	4
ρ_c/Mg m^{-3}	1.428	1.451	1.305
μ/mm^{-1}	2.235	2.502	2.016
F(000)	3000	3016.0	2800
θ range(°)	4.29 to 49.99	4.46 to 50	4.31 to 49.99
reflections collected	46826	81881	23406
Completeness to θ (%)	99.9	99.9	99.6
independent reflections/R_{int}	6019/ 0.0587	5976 /0.0542	5964/0.1724
GooF(F^2)	1.178	1.295	1.005
Final R indices (I>2σ(I))	$R_1 = 0.0508$ $wR_2 = 0.0906$	$R_1 = 0.0453$ $wR_2 = 0.0905$	$R_1 = 0.0869$ $wR_2 = 0.1998$
R indices (all data)	$R_1 = 0.0763$ $wR_2 = 0.1002$	$R_1 = 0.0503$ $wR_2 = 0.0929$	R1 = 0.2168 wR2 = 0.2897

Table S2: Selected bond lengths and bond angles for complexes **1**-**3**.

	1	**2**	**3**
Ln1-Cl1	2.6811(15)	2.6617(13)	2.644(2)
Ln1-Cl2^1	2.6632(18)	2.6224(17)	2.609(3)
Ln1-Cl3	2.649(2)	2.6368(15)	2.636(3)
Ln1-Cl1^1	2.9229(15)	2.8677(13)	2.878(3)
Ln1-O1	2.395(4)	2.370(4)	2.357(6)
Ln1-N1	2.276(5)	2.242(4)	2.241(9)
Cl2-Li1	2.330(15)	2.331(12)	2.34(2)
Cl3-Li1	2.327(16)	2.300(12)	2.31(3)
Li1-O3	1.901(17)	1.976(16)	1.93(2)
Li1-O2	1.962(17)	1.943(13)	1.90(2)
Cl1-Ln1-Cl1^1	77.41(5)	77.46(4)	77.70(8)
Cl2^1-Ln1-Cl1^1	82.37(6)	82.51(5)	83.06(9)
Cl2^1-Ln1-Cl1	94.52(6)	89.96(6)	90.48(9)
Cl3-Ln1-Cl1	82.02(7)	94.16(5)	93.97(8)
Cl3-Ln1-Cl2^1	162.48(7)	163.53(6)	163.94(11)
O1-Ln1-Cl1	82.09(10)	159.46(10)	160.16(18)
O1-Ln1-Cl1^1	158.98(10	82.39(9)	82.73(17)
O1-Ln1-Cl2^1	87.23(13)	83.46(11)	83.86(17)
O1-Ln1-Cl3	82.80(13)	87.19(11)	86.78(17)
N1-Ln1-Cl1	99.55(12)	99.92(11)	99.49(18)
N1-Ln1-Cl1^1	176.95(12)	177.38(11)	177.17(18)
N1-Ln1-Cl2^1	98.09(15)	97.57(13)	97.6(2)
N1-Ln1-Cl3	97.93(15)	144.98(8)	96.9(2)
N1-Ln1-O1	100.94(15)	100.22(14)	100.1(2)
Ln1-Cl1-Ln1^1	102.59(5)	102.54(4)	102.30(8)
Li1-Cl2-Ln1^1	119.1(4)	119.9(3)	120.1(6)
Li1-Cl3-Ln1^1	120.4(4)	119.6(3)	119.7(6)
Cl3-Li1-Cl2	122.4(6)	121.6(5)	121.4(10)
O3-Li1-Cl2	111.0(7)	112.3(7)	98.4(9)
O3-Li1-Cl3	98.3(7)	97.0(5)	98.4(9)
O3-Li1-O2	106.7(7)	111.0(7)	105.5(12)
O3-Li1-Cl2	107.9(7)	107.7(7)	145.04(7)
O2-Li1-Cl3	109.4(7)	110.4(6)	108.8(10

Table S3: Summary of SHAPE analysis for **1 - 3**

S. No.	Geometry	Cshm value for Gd	Cshm value for Dy	Cshm value for Y
1	Hexagon (D6h)	33.107	32.973	33.001
2	Pentagonal pyramid (C5v)	28.343	28.416	28.500
3	Octahedron (Oh)	**0.715**	**0.677**	**0.662**
4	Trigonal prism (D3h)	14.796	14.881	14.906
5	Johnson pentagonal pyramid J2 (C5v)	31.504	31.460	31.543

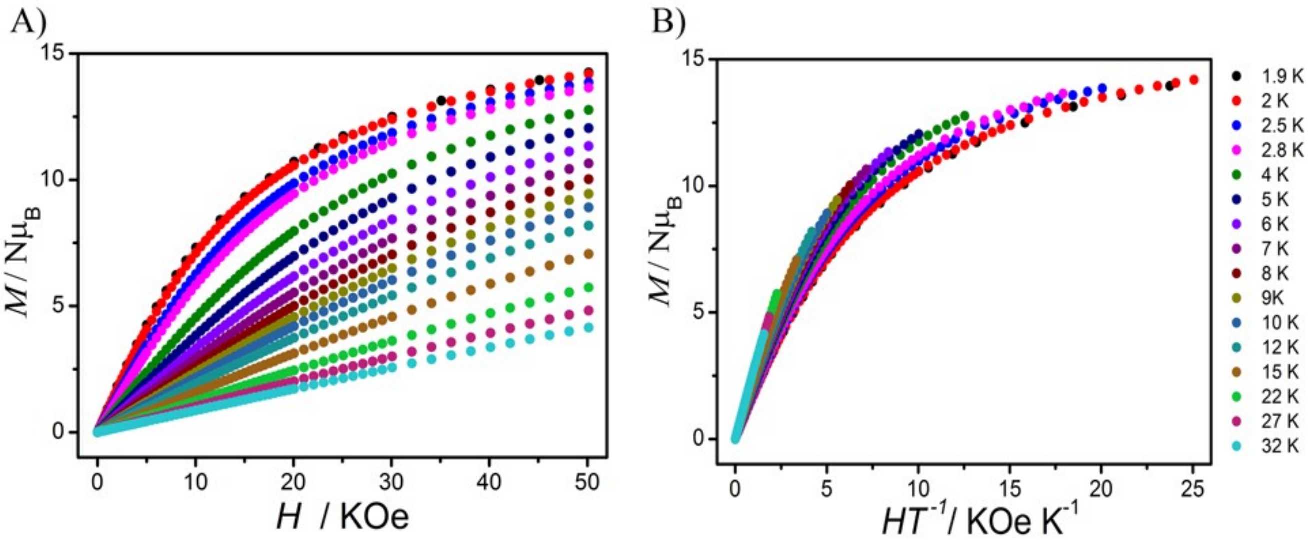

Figure S5: Detailed isothermal field dependent magnetization measurement performed on polycrystalline sample of **1** measured from 0 - 5 Tesla at the indicated temperatures. **B)** Reduced magnetization plots of complex **1**

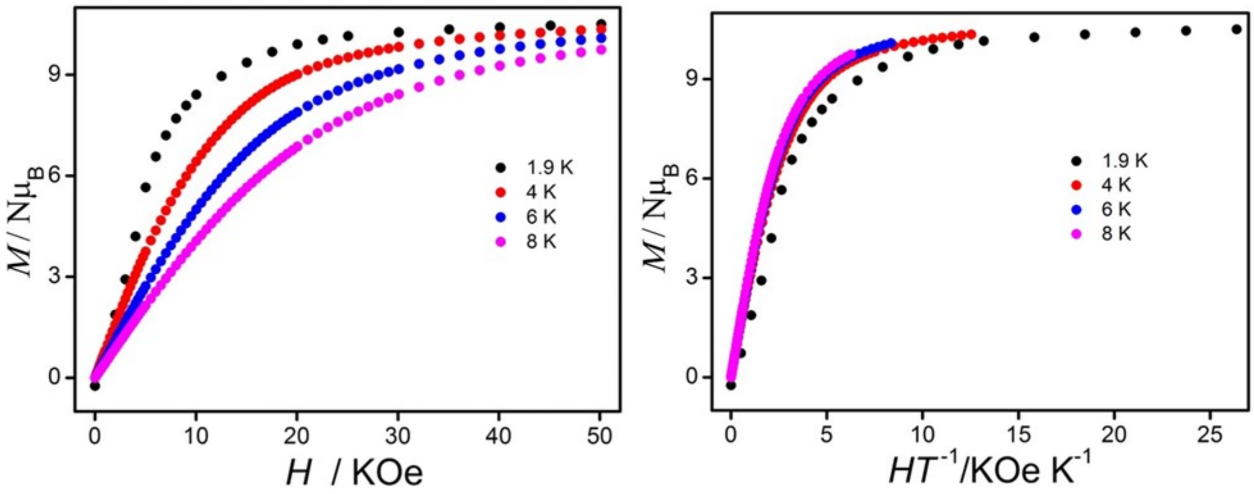

Figure S6: Field dependence of the magnetization plots for polycrystalline sample of **2** measured from 0 - 5 Tesla at the indicated temperatures. **B)** Reduced magnetization plots of complex **2**.

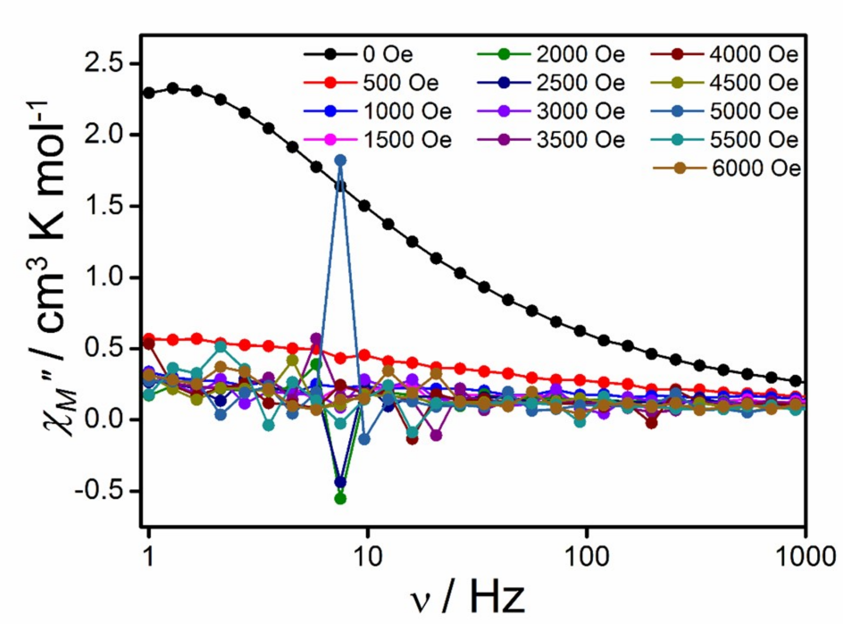

Figure S7: Frequency dependence of the imaginary (χ_M'') components of the ac susceptibility at different ac frequencies from 1 - 1500 Hz and different external dc field from 0 – 6000 Oe, respectively with a 3.5 Oe ac field for **2** at 1.9 K.

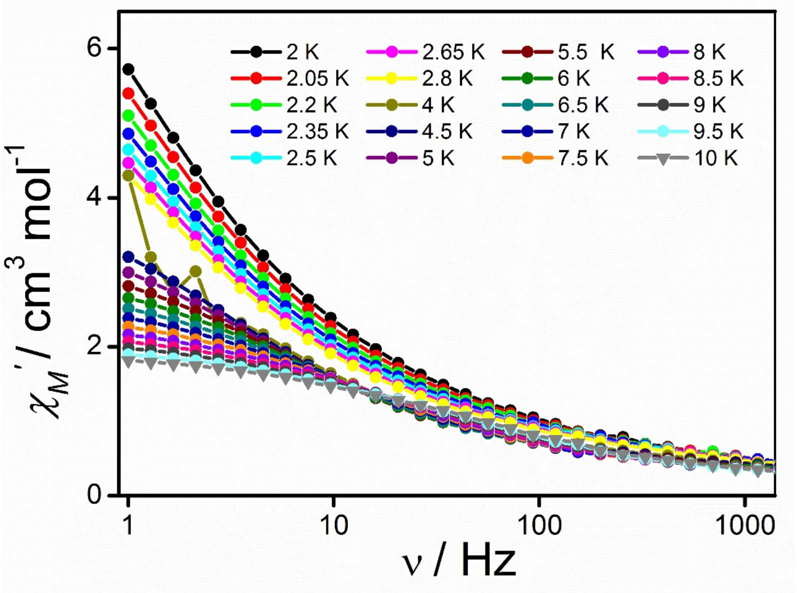

Figure S8: Frequency dependence of the real (χ_M') components of the ac susceptibility at different ac frequencies from 1 - 1500 Hz under 0 Oe external dc field, with a 3.5 Oe ac field for **2** at different temperatures.

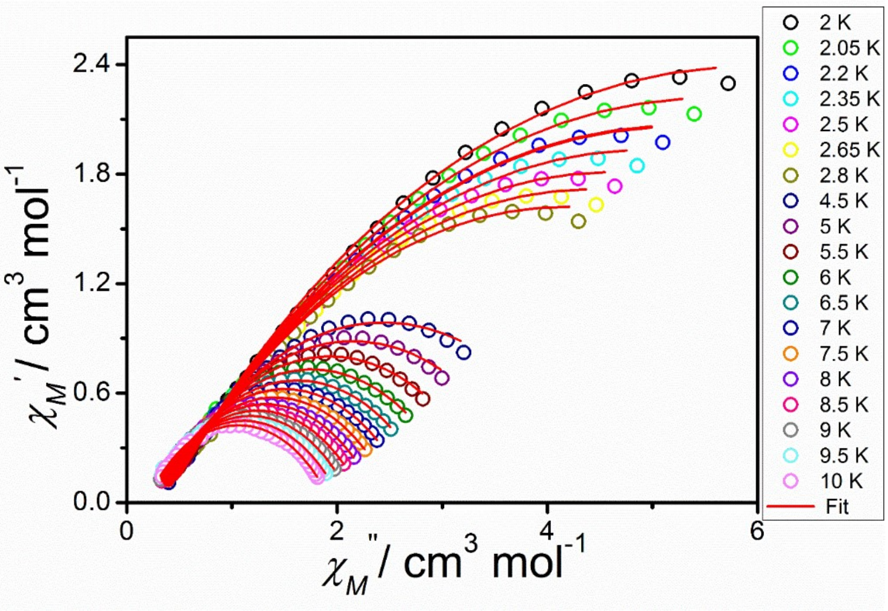

Figure S9: Cole-Cole plot of polycrystalline sample of **2** in the presence of 0 Oe external magnetic field at different temperatures.

Table S4: The best-fitting parameters obtained for Cole-Cole plot of complex **2**

S. No.	**Temperature (K)**	χ_S	χ_T	**τ**	**α**	**Residual**
1	1.9	0.348350E+00	0.114553E+02	0.189943E+00	0.482840E+00	0.956949E-01
2	2.05	0.352627E+00	0.107007E+02	0.185918E+00	0.484736E+00	0.865500E-01
3	2.2	0.352179E+00	0.100335E+02	0.182802E+00	0.487500E+00	0.849988E-01
4	2.35	0.351960E+00	0.945806E+01	0.177760E+00	0.489149E+00	0.838478E-01
5	2.5	0.351243E+00	0.884567E+01	0.165337E+00	0.486793E+00	0.680383E-01
6	2.65	0.337604E+00	0.849947E+01	0.165919E+00	0.492978E+00	0.804193E-01
7	2.8	0.346139E+00	0.798070E+01	0.153184E+00	0.488805E+00	0.745702E-01
8	4.5	0.343073E+00	0.453326E+01	0.543557E-01	0.438977E+00	0.333822E-01
9	5	0.330057E+00	0.396955E+01	0.392222E-01	0.423544E+00	0.225642E-01
10	5.5	0.327308E+00	0.353647E+01	0.292911E-01	0.410065E+00	0.170626E-01
11	6.0	0.304550E+00	0.321140E+01	0.222935E-01	0.406888E+00	0.789772E-02
12	6.5	0.281451E+00	0.295857E+01	0.173747E-01	0.409104E+00	0.711531E-02
13	7	0.274014E+00	0.272878E+01	0.136179E-01	0.402027E+00	0.285339E-02
14	7.5	0.260335E+00	0.255384E+01	0.109451E-01	0.406725E+00	0.307396E-02
15	8	0.236129E+00	0.239842E+01	0.864241E-02	0.410174E+00	0.281504E-02
16	8.5	0.221658E+00	0.226722E+01	0.701012E-02	0.415791E+00	0.302941E-02
17	9	0.204633E+00	0.214848E+01	0.566189E-02	0.420275E+00	0.268900E-02
18	9.5	0.179407E+00	0.204495E+01	0.452530E-02	0.428461E+00	0.428529E-02
19	10	0.179741E+00	0.194581E+01	0.376682E-02	0.429149E+00	0.373496E-02

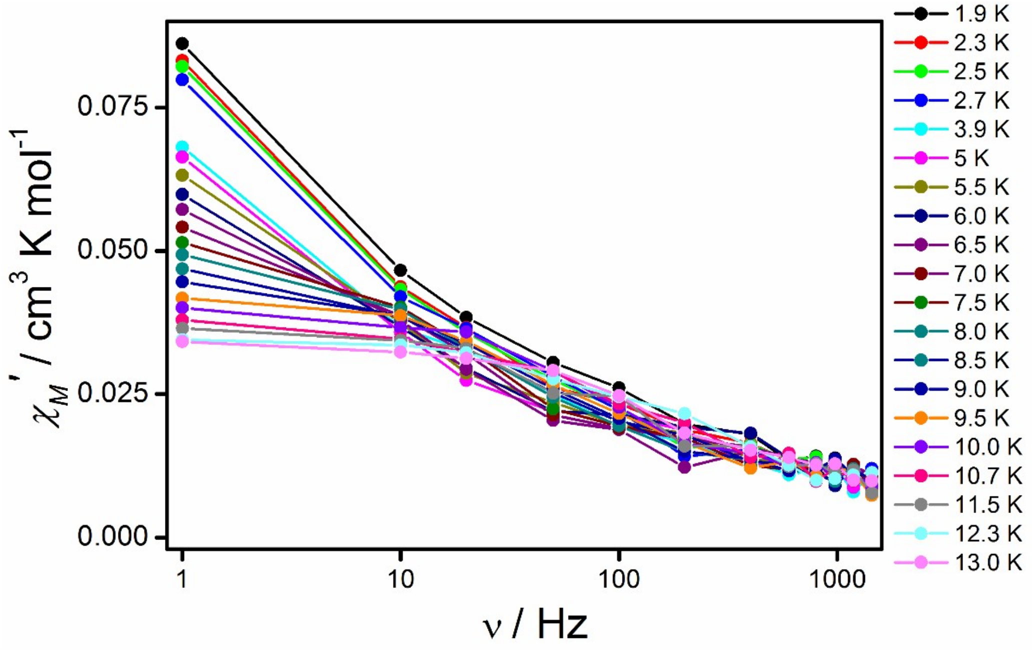

Figure S10: Frequency dependence of the real (χ_M') components of the ac susceptibility at different ac frequencies from 1 - 1500 Hz under 0 Oe external dc field, with a 3.5 Oe ac field for a magnetically diluted sample of **2** (5 %) at different temperatures.

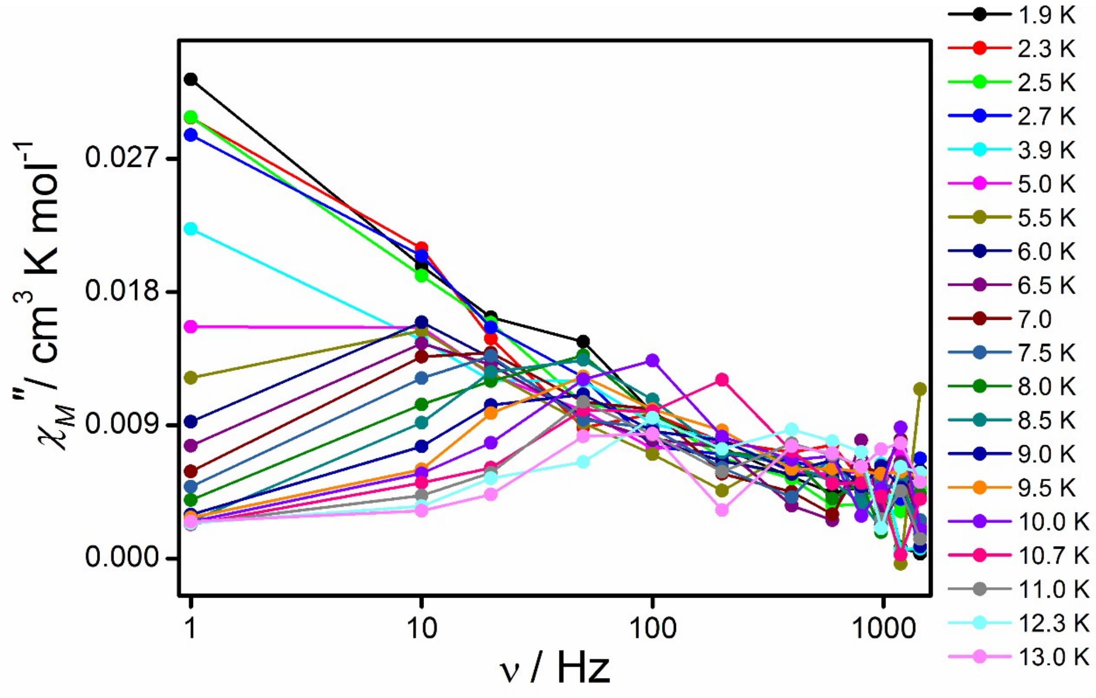

Figure S11: Frequency dependence of the real (χ_M'') components of the ac susceptibility at different ac frequencies from 1 - 1500 Hz under 0 Oe external dc field, with a 3.5 Oe ac field for a magnetically diluted sample of **2** (5 %) at different temperatures.

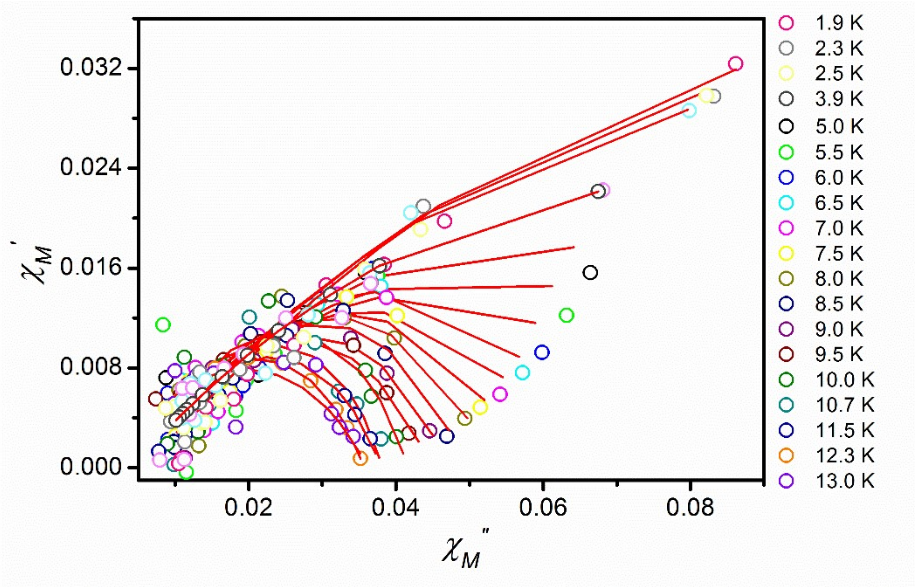

Figure S12 Cole-Cole plot of polycrystalline sample of magnetically diluted sample of **2** (5 %) in the presence of 0 Oe external magnetic field at different temperatures.

Table S5: The best-fitting parameters obtained for the Cole-Cole plot of a magnetically diluted sample of **2** (5 %)

S. No.	Temperature (K)	χ_S	χ_T	τ	α	residual
1.	1.9	6.11E-03	2.27E-01	6.17E-01	6.17E-01	6.84E-05
2.	2.3	4.98E-03	2.12E-01	5.45E-01	6.17E-01	4.80E-05
3.	2.5	6.53E-03	1.88E-01	3.41E-01	5.87E-01	3.37E-05
4.	2.7	4.65E-03	1.92E-01	4.04E-01	6.10E-01	3.64E-05
5.	3.9	1.59E-03	1.90E-01	9.67E-01	6.73E-01	1.96E-05
6.	4.9	6.03E-03	1.10E-01	9.55E-02	5.77E-01	6.61E-05
7.	5.49	4.37E-03	9.60E-02	5.46E-02	5.88E-01	1.25E-04
8.	6	7.26E-03	7.93E-02	2.83E-02	5.30E-01	7.44E-05
9.	6.5	8.55E-03	6.69E-02	1.68E-02	4.27E-01	6.76E-05
10.	7	8.58E-03	6.30E-02	1.19E-02	4.50E-01	6.63E-05
11.	7.5	8.07E-03	5.72E-02	7.93E-03	4.07E-01	3.15E-05
12.	8	8.02E-03	5.29E-02	5.66E-03	3.68E-01	3.12E-05
13.	8.5	8.60E-03	4.92E-02	4.56E-03	3.35E-01	2.49E-05
14.	9	8.45E-03	4.69E-02	3.70E-03	3.53E-01	3.03E-05
15.	9.5	6.09E-03	4.46E-02	2.42E-03	3.68E-01	3.33E-05
16.	10	8.12E-03	4.15E-02	1.95E-03	2.63E-01	5.74E-05
17.	10.7	8.43E-03	3.81E-02	1.54E-03	2.51E-01	4.37E-05
18.	11.47	7.78E-03	3.79E-02	1.69E-03	3.23E-01	5.22E-05
19.	12.23	5.84E-03	3.56E-02	9.00E-04	3.19E-01	3.64E-05

21.	12.90	2.78E-03	3.61E-02	7.20E-04	4.37E-01	4.37E-05

Computational details:

CASSCF calculations on individual Dy^{III} fragmentof the model structure extracted from the compound on the basis of single-crystal X-ray determined geometry have been carried out with MOLCAS 8.0 program package. Single_Aniso program was used to obtain the ***g*** tensors, energy levels and magnetic axes based on the above CASSCF/RASSI calculation. The basis sets for all atoms obtained from the MOLCAS ANO-RCC library:

Table S6: Basis set used for all the elements in our calculation.

element	Basis Set
H	H.ANO-RCC...2s.
C	C.ANO-RCC...3s2p.
N	N.ANO-RCC...4s3p2d.
O	O.ANO-RCC...4s3p2d.
Si	Si.ANO-RCC...3s2p.
Cl	Cl.ANO-RCC...4s3p2d.
Dy	Dy.ANO-RCC...8s7p4d3f2g1h.

Table S7: Calculated energy levels (cm^{-1}), g (g_x, g_y, g_z) tensors of complex **2**.

KDs	**g_x**	**g_y**	**g_z**	**Energy in cm^{-1}**	**θ °**
1	0.03	0.05	19.86	0	0
2	1.46	3.94	14.4	197.25	176.83
3	1.26	4.59	11.37	274.12	94.14
4	3.54	4.70	9.18	379.66	87.00
5	0.628	1.449	15.60	480.92	79.11
6	1.093	1.53	14.35	498.09	99.94
7	0.3757	0.958	16.91	564.75	112.16
8	0.0188	0.0584	19.05	630	68.39

Table S8: SINGLE_ANISO computed crystal field parameter of complex **2**.

k	**q**	B_k^q

2	-2	-0.80E+00
	-1	0.74E+00
	0	**-0.24E+01**
	1	-0.50E+00
	2	0.21E+01
4	-4	-0.22E-02
	-3	0.67E-02
	-2	-0.14E-02
	-1	-0.38E-02
	0	-0.86E-02
	1	0.33E-02
	2	0.41E-02
	3	0.84E-03
	4	**-0.36E-01**
6	-6	0.65E-05
	-5	-0.20E-03
	-4	-0.27E-04
	-3	0.21E-04
	-2	0.54E-04
	-1	-0.50E-07
	0	0.27E-04
	1	0.17E-05
	2	-0.83E-04
	3	-0.36E-04
	4	-0.17E-03
	5	0.20E-03
	6	0.50E-04

$$\hat{H}cf = \sum \sum_{K=-q}^{q} B_k^q \, \tilde{O}_k^q \qquad \text{………(1)}$$

Where B_k^q represents the crystal field parameter and $\tilde{O}_k^q$ represents the Stevens operator.

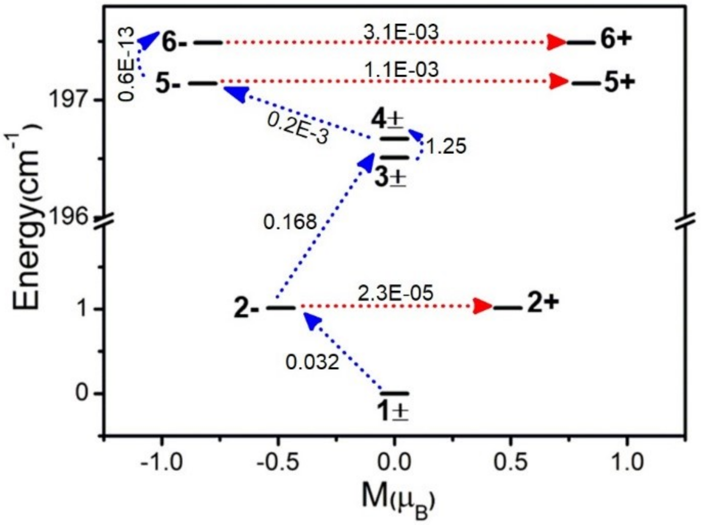

Figure S13: The low-lying exchange spectrum and magnetization blocking barrier of complex **2**.

References:

1 D.A. Gaul, O. Just, W.S. Rees Jr., *Inorg. Chem*. 2000, **19**, 5648.

2. D. B. G. Williams and M. Lawton, *J. Org. Chem.* 2010, **75**, 8351.

3. G. Sheldrick, *Acta Crystallogr. Sect.C.* 2015, **71**, 3.

4. (a) S. Alvarez, P. Alemany, D. Casanova, J. Cirera, M. Llunell, D. Avnir, *Coord. Chem. Rev.* 2005, **249**, 1693. (b) D. Casanova, M. Llunell, P. Alemany, S. Alvarez, *Chem. –Eur. J*. 2005, **11**, 1479.